CFSRC COLLOQUIUM

Proceedings of the Cold-Formed Steel Research Consortium Colloquium
17-19 October 2022 (cfsrc.org)

Global Buckling Analysis of Tapered Steel Members with Nonsymmetric Sections via an Updated-Lagrangian Line-Element Formulation

A.H.A. Abdelrahman[1], S. Lotfy[2], and Siwei Liu[3]

Abstract

With the advancement in manufacturing technology, fabricating nonsymmetric steel sections by cold-forming or robotic welding is feasible, enabling innovative structural forms of being more structurally efficient. Nevertheless, members with nonsymmetric sections usually experience complex behaviour such as torsional, flexural-torsional, and lateral-torsional buckling, complicating their buckling strength prediction. The line-element method is proven efficient and robust for the stability analysis of framed structures. This paper develops a new tapered line-element suiting for nonlinear elastic buckling analysis of steel structures comprising tapered members with nonsymmetric sections. The approximate prediction of the varied cross-sectional properties along the length via the tapered variability indexes shows more accurate results than the stepped-element representation approach. Extensive parametric studies are conducted for the geometric parameters of typical shapes of nonsymmetric sections. The element tangent stiffness matrix, compatible with the existing frame analysis programs, is derived via the total potential energy principle. Moreover, the numerical procedure of the proposed method via the Updated-Lagrangian (UL) approach is elaborated and validated through several benchmark examples generated by shell-finite elements. Finally, the practical application of the proposed method is explored. This paper provides a new line element for a nonlinear elastic analysis to examine global buckling behaviours that represent an initial basis for forthcoming nonlinear collapse simulations with imperfections that are the primary goals in future studies.

1. Introduction

Modern construction technologies are recently used in fabricating nonsymmetric steel shapes being tapered along the length. Tapered steel members are often employed in multi-story buildings, sloped frames, and bridges due to their tendency to be highly optimized. The highly appreciated advantages of tapered members with nonsymmetric sections (TNS), such as structural efficiency and material savings, facilitate their applications in contemporary structures. A major feature of nonsymmetric sections is that the shear center and the cross-sectional centroid do not coincide, thereby imposing additional torque when loads are applied to the centroid of the cross-sections [1-4].

Nowadays, modern design methods such as the direct analysis method (DAM) are increasingly used to assess the structural safety of steel constructions. Several techniques are employed to analyze and design tapered members, and they are mainly based on exact analytical solutions or numerical methods. The former is usually applicable for elastic buckling behaviours of individual members with idealized boundary conditions in accordance with the effective length and stiffness reduction approaches [5-9]. On the other side, the FE method employing solid-, shell-, or line elements to discretize tapered members is utilized to simulate the buckling behaviour.

The line finite element method (LFEM) is more appropriate in the frame of a more advanced system-based analysis (i.e., the DAM). The stepped element representation approach and the tapered element approach are usually utilized for modelling structures comprising tapered members. The tapered element representation approach considers the cross-section variation in the element formulation either by the exact analytical expressions [10-14] or approximate distributions [15]. The simplified but sufficiently accurate expressions of the tapered section stiffness factors within the element tangent stiffness matrix can ease the implementation of the tapered element within available structural software and provide a generalized solution for tapered members with arbitrary cross-sections. Thus, the approximate distribution technique is adopted in the current study to provide a generalized approach for analyzing tapered steel members.

Based on recent research on the buckling behavior of steel members with nonsymmetric sections [4, 16-19], it is postulated that the consideration of warping deformations, Wagner effects, and the misalignment of the cross-sectional centroid and the shear center is paramount, thereby improving the accuracy of simulating buckling behavior of nonsymmetric sections under positive or negative bending moments, as shown in Figure 1.

[1]*Lecturer, Structural Engineering Department, Faculty of Engineering, Mansoura University, Egypt.*
[2]*Ph.D, Civil Engineering Department, Misr Higher Institute for Engineering and Technology, Egypt.*
[3]*Associate Professor, Department of Civil and Environmental Engineering, The Hong Kong Polytechnic University, Hong Kong, China.*

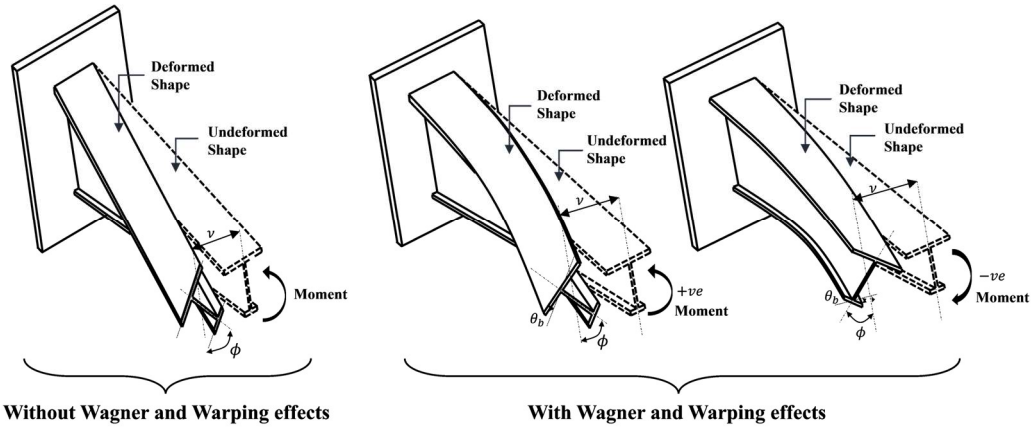

Figure 1. Illustration of buckling behaviours of tapered members with nonsymmetric section

Although earlier studies have considered LTB of tapered monosymmetric I-sections in tapered elements, to the best of the author's knowledge, beam formulations for TNS that count for sections being nonsymmetric, warping deformations, and Wagner effects are limited. Therefore, this research introduces a generalized line-element formulation for tapered steel members with nonsymmetric sections (TNL, as they will be henceforth called). The derivation includes the axial and transverse elastic strains, warping deformations, and Wagner effects. Simplified approximate equations describing the variation of cross-sectional properties along the element are proposed comprising the geometric parameters of common nonsymmetric sections, including T-, L-, mono-symmetric-I, and hollow trapezoidal cross-sections. The proposed TNL element with fewer elements to simulate the member shows a significant numerical efficiency with acceptable accuracy, as indicated by validation and illustrative examples.

2. Geometric Parameters for Nonsymmetric Sections

The present element formulation is derived for nonlinear buckling analysis of tapered steel members with nonsymmetric cross-sections. Thus, a parametric study is conducted by the authors [20] for typical sectional shapes with wide ranges of cross-sectional and tapered parameters that describe the cross-section variability via depth, breadth, and both (depth and breadth). Accordingly, the variability of a general section property (ψ) is expressed for a tapered member by,

$$\psi(\xi) = \psi_L\left[1 + \left(\nu_\psi - 1\right)\xi\right]^{n_\psi} \quad (1)$$

where ψ is the section property under consideration; ν_ψ is the tapering ratio $\left(= \sqrt[n_\psi]{\psi_R/\psi_L}\right)$; ψ_L and ψ_R are the section property at $\xi = 0$ and $\xi = 1$, as presented in Figure 2; and n_ψ is the variability index corresponding to the section property ψ, as tabulated in Table 1.

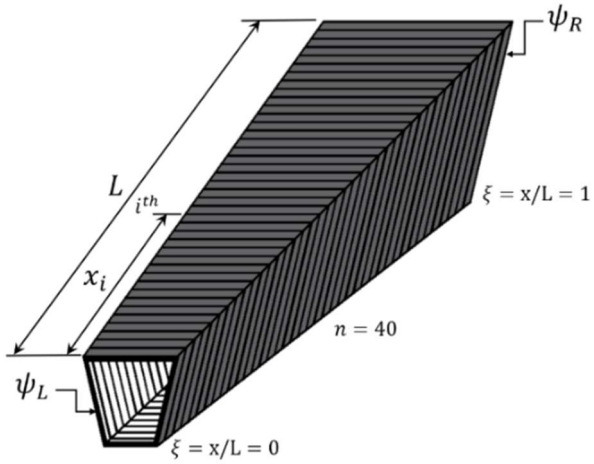

Figure 2. Typical tapered parameters and interval points along the member

Table 1. Values of tapered variability indexes for different section types.

Section type	Varying breadth only (VB)			Varying depth only (VD)			Both (VBD)		
	n_{Iz}	n_{Iy}	n_{Iw}	n_{Iz}	n_{Iy}	n_{Iw}	n_{Iz}	n_{Iy}	n_{Iw}
TMI, THT, TL, and TT	1	3	3	2.5	1	2	3	3	4.5

In conclusion, Table 2 summarizes the different section properties adopted by the variability index and the averaging values methods.

Table 2. Summary of the section properties adopted by each method.

Variability index	Averaging values
• Moment of inertia about the y-axis (I_y), and about the z-axis (I_z). • Warping constant (I_w).	• Area (A), Torsional rigidity (J). • Shear center coordinates (Y_s, Z_s) • Wagner coefficients (β_z, β_y and β_ω)

3. Beam-column Element Formulation

3.1 Assumptions and definitions

The present element formulation for tapered members with nonsymmetric sections assumes that; 1) the Updated-Lagrangian method is adopted for relatively large deflections; 2) material is linearly elastic and obeys Hooke's law; 3) loads are conservative; 4) shear deformations are ignored, and 5) local and distortional buckling are not considered.

The nodal axial displacement (u), lateral displacements (v and w), rotations (θ) about the element's local x, y, and z-axes, and the warping deformations (θ_b) are given respectively representing the element's degrees of freedom (DOFs) [Δ] as,

$$[\Delta] = [u_1\ v_1\ w_1\ \theta_{x1}\ \theta_{y1}\ \theta_{z1}\ \theta_{b1}\ \ u_2\ v_2\ w_2\ \theta_{x2}\ \theta_{y2}\ \theta_{z2}\ \theta_{b2}] \tag{2}$$

3.2 Interpolation functions for element deformation shapes

The axial and lateral deformations along the element length $[d_o]$ can be described by the interpolated polynomials in terms of the element's nodal deformations [Δ] as follow,

$$[d_o] = [u_o\ \ v_o\ \ w_o\ \ \theta_x]^T = [N][\Delta]^T \tag{3}$$

where u_o is the axial displacement along the element length; v_o and w_0 denote the lateral displacements along the sectional y- and z-axes; θ_x is the twist rotation; and [N] is the shape function matrix and defined as,

$$[N] = \begin{bmatrix} N_1 & 0 & 0 & 0 & 0 & 0 & 0 \\ 0 & N_4 & 0 & 0 & 0 & N_5 & 0 \\ 0 & 0 & N_4 & 0 & -N_5 & 0 & 0 \\ 0 & 0 & 0 & N_4 & 0 & 0 & N_5 \\ N_2 & 0 & 0 & 0 & 0 & 0 & 0 \\ 0 & N_3 & 0 & 0 & 0 & -N_6 & 0 \\ 0 & 0 & N_3 & 0 & N_6 & 0 & 0 \\ 0 & 0 & 0 & N_3 & 0 & 0 & -N_6 \end{bmatrix} \tag{4}$$

in which (N_1 to N_6) are the shape function coefficients given at any section whose coordinate parameter $\xi(= x/L)$ as: $N_1 = 1-\xi$, $N_2 = \xi$, $N_3 = 3\xi^2 - 2\xi^3$, $N_4 = 1 - 3\xi^2 + 2\xi^3$, $N_5 = x(1 - 2\xi + \xi^2)$, and $N_6 = x(\xi - \xi^2)$.

3.4 Total potential energy

The total potential energy function is expressed by subtracting the external work done by the element V from the stored strain energy U. The strain energy that comprises the linear and nonlinear portions of the stress-strain constitutive relationship can be expressed as follow,

$$U = \frac{1}{2}\int_V \left([\sigma]^T[\varepsilon]\right)dv \tag{5}$$

By substituting the Green-Lagrange strain tensor and the normal and shear stresses acting on the cross-section into Eq. (5), the potential strain energy can be expressed in its simple form as,

$$\begin{aligned} U \approx{}& \frac{1}{2}\int_0^L \left[\begin{array}{l} E\bar{A}\left(\frac{\partial u_o(x)}{\partial x}\right)^2 + EI_z(x)\left(\frac{\partial \theta_z(x)}{\partial x}\right)^2 + EI_y(x)\left(\frac{\partial \theta_y(x)}{\partial x}\right)^2 \\ +EI_w(x)\left(\frac{\partial^2 \theta_x(x)}{\partial x^2}\right)^2 + G\bar{J}\left(\frac{\partial \theta_x(x)}{\partial x}\right)^2 \end{array} \right] dx \\ &+\frac{1}{2}\int_0^L P\left[\left(\frac{\partial v_o(x)}{\partial x}\right)^2 + \left(\frac{\partial w_o(x)}{\partial x}\right)^2\right]dx + \frac{1}{2}\int_0^L Pr^2\left(\frac{\partial \theta_x(x)}{\partial x}\right)^2 dx \\ &+\frac{1}{2}\int_0^L P\left(2\bar{Y}_s\frac{\partial w_o(x)}{\partial x} - 2\bar{Z}_s\frac{\partial v_o(x)}{\partial x}\right)\frac{\partial \theta_x(x)}{\partial x}dx \\ &+M_{y1}\int_0^L \frac{L-x}{L}\frac{\partial \theta_x(x)}{\partial x}\left[\frac{\partial v_o(x)}{\partial x} + \frac{1}{2}\bar{\beta}_y\frac{\partial \theta_x(x)}{\partial x}\right]dx - \\ &M_{y2}\int_0^L \frac{x}{L}\frac{\partial \theta_x(x)}{\partial x}\left[\frac{\partial v_o(x)}{\partial x} + \frac{1}{2}\bar{\beta}_y\frac{\partial \theta_x(x)}{\partial x}\right]dx \\ &+M_{z1}\int_0^L \frac{L-x}{L}\frac{\partial \theta_x(x)}{\partial x}\left[\frac{\partial w_o(x)}{\partial x} + \frac{1}{2}\bar{\beta}_z\frac{\partial \theta_x(x)}{\partial x}\right]dx - \\ &M_{z2}\int_0^L \frac{x}{L}\frac{\partial \theta_x(x)}{\partial x}\left[\frac{\partial w_o(x)}{\partial x} + \frac{1}{2}\bar{\beta}_z\frac{\partial \theta_x(x)}{\partial x}\right]dx \\ &+V_y\int_0^L\left[\left(\theta_x(x)\frac{\partial w_o(x)}{\partial x} - \frac{\partial u_o(x)}{\partial x}\frac{\partial v_o(x)}{\partial x}\right)\right]dx - \\ &V_z\int_0^L\left[\left(\theta_x(x)\frac{\partial v_o(x)}{\partial x} + \frac{\partial u_o(x)}{\partial x}\frac{\partial w_o(x)}{\partial x}\right)\right]dx \\ &+\frac{1}{2}\int_0^L M_b\bar{\beta}_\omega\left(\frac{\partial \theta_x(x)}{\partial x}\right)^2 \end{aligned} \tag{6}$$

where $E\bar{A}$, and $G\bar{J}$ represent the axial stiffness, and torsion rigidity, respectively; $EI_z(x)$, $EI_y(x)$, and $EI_w(x)$ are,

respectively, the variation of flexural stiffness about the z- and y-axis and the warping rigidity along the element length, which are calculated based on the tapered variability factors in Table 1; $\overline{Y_s}$, $\overline{Z_s}$, $\overline{\beta_y}, \overline{\beta_z}$, and $\overline{\beta_\omega}$ are the averaged shear center coordinates and Wagner's coefficients; r^2 can be calculated by, $r^2 = \left[\bar{I}_y + \bar{I}_z\right]/\bar{A}$. For more details the reader is referred to [20].

3.4 Tangent stiffness matrix

The second variation of the total potential energy yields the element's tangent stiffness matrix for the tapered warping element being expressed as,

$$\left[k\right]_e = [T]\left(\left[k_L\right] + \left[k_G\right] + \left[k_U\right]\right)[T]^T \tag{7}$$

where $[k_L]$ is the linear elastic stiffness matrix and $[k_G]$ is the geometric stiffness matrix provided by McGuire, et al. [21], and the additional geometric stiffness matrix $[k_U]$, which is provided by Liu, et al. [19] to account for nonsymmetrical section-effects. While the transformation matrix $[T]$ transforms the element's local axis to reference the cross-sectional centroid given by McGuire, et al. [21].

The proposed linear stiffness matrix $[k_L]$ that accounts for the variation of the cross-sectional properties for tapered members are given as follows,

$$[k_L] = \begin{bmatrix}
\frac{E\bar{A}}{L} & 0 & 0 & 0 & 0 & 0 & 0 & -\frac{E\bar{A}}{L} & 0 & 0 & 0 & 0 & 0 & 0 \\
 & \alpha_{z1} & 0 & 0 & 0 & \alpha_{z2} & 0 & 0 & -\alpha_{z1} & 0 & 0 & 0 & \alpha_{z3} & 0 \\
 & & \alpha_{y1} & 0 & -\alpha_{y2} & 0 & 0 & 0 & 0 & -\alpha_{y1} & 0 & -\alpha_{y3} & 0 & 0 \\
 & & & \beta_1 & 0 & 0 & \beta_2 & 0 & 0 & 0 & -\beta_1 & 0 & 0 & \beta_3 \\
 & & & & \alpha_{y4} & 0 & 0 & 0 & 0 & \alpha_{y2} & 0 & \alpha_{y5} & 0 & 0 \\
 & & & & & \alpha_{z4} & 0 & 0 & -\alpha_{z2} & 0 & 0 & 0 & \alpha_{z5} & 0 \\
 & & & & & & \beta_4 & 0 & 0 & 0 & -\beta_2 & 0 & 0 & \beta_5 \\
 & & S. & & & & & \frac{E\bar{A}}{L} & 0 & 0 & 0 & 0 & 0 & 0 \\
 & & & Y. & & & & & \alpha_{z1} & 0 & 0 & 0 & -\alpha_{z3} & 0 \\
 & & & & M. & & & & & \alpha_{y1} & 0 & \alpha_{y3} & 0 & 0 \\
 & & & & & & & & & & \beta_1 & 0 & 0 & -\beta_3 \\
 & & & & & & & & & & & \alpha_{y6} & 0 & 0 \\
 & & & & & & & & & & & & \alpha_{z6} & 0 \\
 & & & & & & & & & & & & & \beta_6
\end{bmatrix} \tag{8}$$

where $\alpha_{j1} = 36Ek_{j1}/L^3$, $\alpha_{j1} = 12Ek_{j2}/L^2$, $\alpha_{j3} = 12Ek_{j3}/L^2$, $\alpha_{j4} = 4Ek_{j4}/L$, $\alpha_{j5} = 4Ek_{j5}/L$, $\alpha_{j6} = 4Ek_{j6}/L$, $\beta_1 = 36Ek_{w1}/L^3 + 6G\bar{J}/5L$, $\beta_2 = 12Ek_{w2}/L^2 + G\bar{J}/10$, $\beta_3 = 12Ek_{w3}/L^2 + G\bar{J}/10$, $\beta_4 = 4Ek_{w4}/L + 2G\bar{J}L/15$, $\beta_5 = 4Ek_{w5}/L - G\bar{J}L/30$, $\beta_6 = 4Ek_{w6}/L + 2G\bar{J}L/15$; and k_{ji} is the tapering linear stiffness factors and given in Appendix I. As a sequel, the five section properties (Y_s, Z_s, β_y, β_z, and β_ω) basically included within the geometrical stiffness matrices (i.e., $[k_G]$ and $[k_U]$) are replaced by the averaging corresponding properties ($\overline{Y_s}$, $\overline{Z_s}$, $\overline{\beta_y}, \overline{\beta_z}$, and $\overline{\beta_\omega}$).

3.5 Formation of global tangent stiffness

Based on the calculated tangent stiffness matrix for a number of elements (NELE) comprising the structural system, the global stiffness matrix with reference to a single global coordinate system is assembled and calculated by,

$$\left[k\right]_g = \sum_{i=1}^{NELE} [\Omega]^T [k]_e^i [\Omega] \tag{9}$$

Where $[\Omega]$ is a transformation matrix of the element's local coordinate system to a single global system, which needs to be updated during each analysis load increment as per McGuire, et al. [21].

4. Numerical implementation

The most relevant procedures and the numerical implementation of the proposed TNL elements are addressed in this section. In particular, the issues discussed include the modelling of tapered members and the numerical technique involved in the analysis. At first, structures are described by a number of tapered members interconnected at nodes. The start and end sections of tapered members are defined as per the cross-section analysis algorithm within MASTAN2 [22]. Accordingly, the cross-sections at the interval points along the elements are automatically defined wherein the sectional properties are calculated. As such, the averaged values of advanced properties needed for nonsymmetric sections (i.e., $\bar{Y}_s$, $\bar{Z}_s$, $\bar{\beta}_y$, $\bar{\beta}_z$, and $\bar{\beta}_\omega$) are calculated. Afterwards, the incremental-iterative procedure adopting the incremental force as unbalanced forces are started. At each incremental step, the element's tangent stiffness matrix is calculated based on nodal displacements and element forces and employing tapered stiffness via the tapered variability indexes in Table 1.

Furthermore, the Updated Lagrangian (UL) approach is introduced to track the nonlinear behaviour during an incremental analysis. The Newton-Raphson technique is utilized for large deflection analysis, yielding the equilibrium conditions at each incremental step. The stiffness matrix is updated as a sequel, and the global stiffness matrix is reassembled. Figure 3 summarizes the proposed computational procedures and the employed incremental-iterative technique of the TNL elements.

5. Validation and illustrative example

The validation and verification of the proposed element, comparisons of linear and nonlinear buckling results are

conducted based on results obtained from; 1) the numerical implementation of the proposed 1-D model (TNL elements), 2) the ABAQUS shell FE models (SFEM), and 3) stepped-line elements approach using conventional warping line elements for prismatic members within MASTAN2 [22] and the warping element B31OS in ABAQUS. It is worth mentioning that the B31OS element in ABAQUS does not consider Wagner's effect. Further, there are two elements available in MASTAN2 for line FE simulations. The basic one assumes the section is symmetric and ignores Wagner's effect (called Sym.), and the second (i.e., advanced) considers Wagner's effect and introduces the nonsymmetric section assumptions (called Nonsymm.).

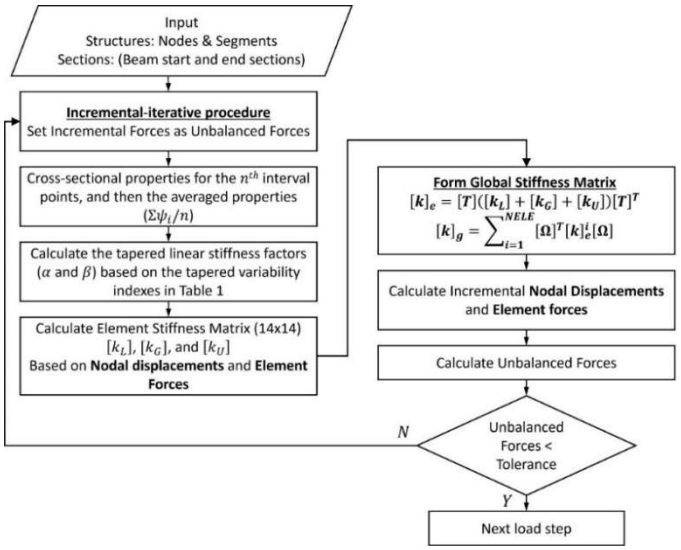

Figure 3. Illustration of the Incremental-iterative procedures for the TNL element

5.1 Eigen buckling analysis of tapered members with nonsymmetric

This example examines the proposed TNL element for bifurcation (Eigen buckling) analysis of a web-tapered T-section cantilever analyzed by Yuan, et al. [23]. The overall width and depth of the cross-section at the fixed end are 100 mm and 260 mm, respectively, while the web and flange thicknesses are 10 mm. The tapering angle α as shown in Figure 4, is 2.5^o making the free-end cross-section's depth varies with respect to the member length being varied from 1.5 to 5.5 m. With a focus on the lateral-torsional buckling (LTB) of the tapered cantilever beam, the elastic LTB moments are plotted versus the cantilever length, as shown in Figure 4. The results obtained from the analytical method and the FE models by Yuan, et al. [23] are plotted together with the results from the proposed TNL element employing four elements to model the beam, and from 30 stepped line elements for prismatic members within MASTAN2 [22]. In addition, results generated from the shell FE models (SFEM) are depicted as benchmark solutions. It can be seen that the proposed TNL element can precisely predict the elastic LTB moments of the cantilever beams with almost identical results when compared to the FE models by Yuan, et al. [23], SFEM, and finely-meshed stepped line elements. In comparison, the analytical solutions in [23], wherein the warping deformations are not considered, overpredict the elastic LTB moments. Notwithstanding, results from the TNL elements for the shorter beam of 1.5 m show conservative results, as observed in Figure 4. That could be attributed to the shear deformations included in the shell FE models are not considered within the proposed line elements.

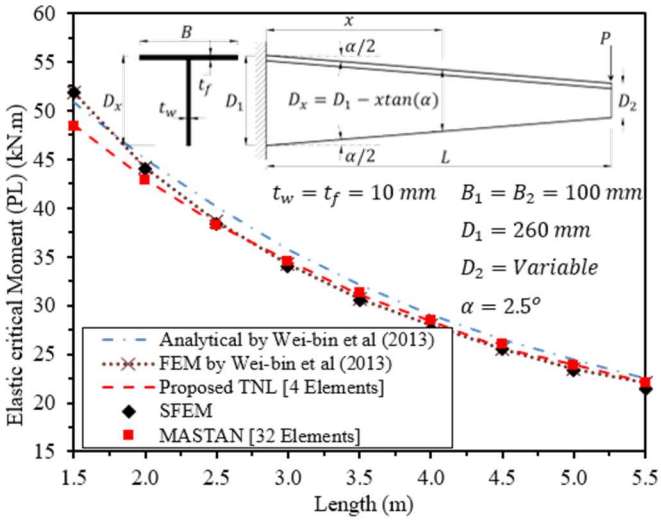

Figure 4. Comparisons of LTB buckling critical moments for a tapered T-section member with a point load at the free end

5.2 Nonlinear analysis of a simply-supported tapered beam with mono-symmetric I-section

In this example, the nonlinear analysis, which considers geometrical nonlinearities, is conducted for simply supported TMI beams under positive and negative bending moments. The lower and upper flange widths are varied from 250 to 150 mm and 500 to 300, respectively, from the left to right end sections. At the same time, the overall depth is varied from 600 mm at the left end section to 400 mm at the right end section. The web and flange thicknesses are kept constant as 30 mm. The beam span is $L = 10.0\ m$, as shown in Figure 5. An initial out-of-straightness with an amplitude of L/1000 is imposed for the intermediate nodes for line element simulations, where L represents the member length. Meanwhile, the first eigenmode is scaled with the same amplitude to trigger the initial geometric imperfections in shell FE models (SFEM). Accordingly, the mid-span lateral displacements are plotted versus the absolute values of applied moments, as shown in Figure 5. It can be seen that the proposed TNL elements employing only four elements per member predict the LTB behaviour of tapered beams with monosymmetric I-section under positive or negative bending moments. Good agreements are clearly

observed with the results obtained from shell FE models and 32 stepped line elements (Nonsymm.). However, the slight discrepancies between the shell and line FE results can be attributed to the different techniques utilized for modelling the geometrical imperfections. On the other side, finely meshed stepped line elements ignoring Wagner's effects (i.e., B31OS and MASTAN2 (Sym.)) cannot predict the LTB behaviour for nonsymmetric sections. These results reconfirm the efficiency of the proposed TNL elements for modelling tapered members with nonsymmetric sections.

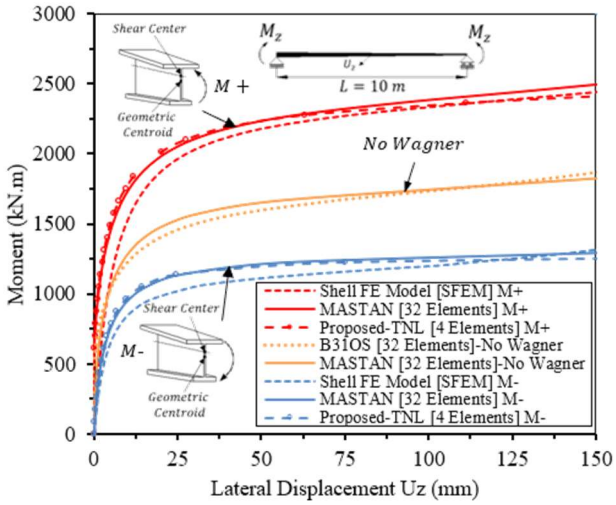

Figure 5. Load versus mid-span lateral displacements for Mono-I beams under uniform bending

5.3 Nonlinear analysis of a single-span portal frame with tapered members

This example further examines the proposed TNL element for a second-order elastic analysis of a single-span portal frame comprised of tapered members with hollow trapezoidal sections. The geometric configurations, the tapering scenario, and cross-sections' dimensions are plotted in Figure 6. The portal frame is assembled utilizing three different tapered members (i.e., members (1), (2), and (3)), as seen in Figure 6. Young's modulus and Poisson's ratio are, respectively, $205\,MPa$ and 0.3. The frame is subjected to a concentrated vertical force at the apex, F, and a lateral force at the eave, $0.2F$. The plane frame is adequately out-of-plane restrained and thereafter analyzed utilizing the proposed tapered element approach and the conventional stepped element method.

Results obtained from 2 proposed TNL elements to model the tapered members (12 elements to model the portal frame) are compared with those obtained from conventional warping nonsymmetric elements within MASTAN2 employing 2, and 30 stepped elements per member (i.e., 12 and 180 elements for the frame). The vertical displacements at the apex point are plotted versus the applied load F, as shown in Figure 6. It is observed that the frame sustains a large deflection at the apex point, which is greater than 2.0 m. In addition, results from only two proposed TNL elements are almost identical to those from finely-meshed stepped elements (30 elements/member). It is clearly seen that two-stepped elements within MASTAN2 cannot predict the large deflection behaviour of portal frames comprising tapered members; even different trends are noted, as shown in Figure 6, especially when the deflection is large. Load-deflection curves in Figure 6 show the robustness and accuracy of the proposed method in analyzing and designing of steel structures comprising tapered members with nonsymmetric sections.

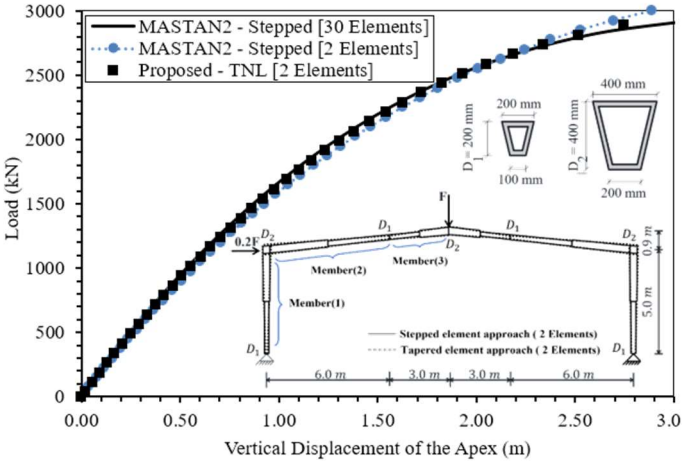

Figure 6. Vertical displacements at the Apex point

6. Conclusions

A new generalized beam-column element, namely TNL, is proposed for direct analysis of steel structures that comprise tapered members with nonsymmetric sections. The warping deformations and Wagner effects are considered, and the nonsymmetric section assumption is introduced. The total potential energy function is utilized to derive the element stiffness matrix composed of tapering section stiffness factors. Simplified approximate expressions are introduced to accurately describe the cross-section variations along the element length via tapered-variability indexes. The detailed numerical implementation is elaborated in a flowchart. Verification and validation of the proposed element are provided using several examples, whereas the accuracy and robustness of the TNL element are established. Comparisons with finely-meshed conventional stepped warping elements and sophisticated shell FE models are demonstrated. Based on the results provided in the current paper, the following conclusions can be drawn.

- When using the proposed approximate equations for the variation of cross-sectional properties along element length, easier implementation of the

proposed element in existing structural software is established and effectively applied for tapered members with arbitrary nonsymmetric sections.

- Results from shell elements show that Wagner effects for nonsymmetric sections continue to be significant when determining the LTB strength of tapered beams under positive or negative bending moments.
- As is consistent with previous studies by the authors on prismatic members with nonsymmetric sections, the consideration of warping deformations, Wagner effects, and misalignment of the shear center and the centroid is essential when an advanced direct analysis method is to be adopted using line FE.

7. Appendix I. Tapered section stiffness factors for nonsymmetrical sections

$$k_{j1} = C_j \begin{pmatrix} n_{Ij}^{\,2}\left(-1+\nu_{Ij}\right)^2\left(-1+\nu_{Ij}^{\,1+n_{Ij}}\right) \\ +n_{Iy}\left(-1+\nu_{Ij}\right)\left(1-5\nu_{Ij}-5\nu_{Ij}^{\,1+n_{Ij}}+\nu_{Ij}^{\,2+n_{Ij}}\right) \\ +2\left(-1-3\nu_{Ij}^{\,2}+3\nu_{Ij}^{\,1+n_{Ij}}+\nu_{Ij}^{\,3+n_{Ij}}\right) \end{pmatrix}$$

$$k_{j2} = C_j \begin{pmatrix} n_{Ij}^{\,2}\left(-1+\nu_{Ij}\right)^2\left(-2+\nu_{Ij}^{\,1+n_{Ij}}\right) \\ -n_{Ij}\left(-1+\nu_{Ij}\right)\left(-3+10\nu_{Ij}+5\nu_{Ij}^{\,1+n_{Ij}}\right) \\ +3\left(-1+\nu_{Ij}-4\nu_{Ij}^{\,2}+2\nu_{Ij}^{\,1+n_{Ij}}+\nu_{Ij}^{\,2+n_{Ij}}+\nu_{Ij}^{\,3+n_{Ij}}\right) \end{pmatrix}$$

$$k_{j3} = C_j \begin{pmatrix} n_{Ij}^{\,2}\left(-1+\nu_{Ij}\right)^2\left(-1+2\nu_{Ij}^{\,1+n_{Ij}}\right) \\ +n_{Ij}\left(-1+\nu_{Ij}\right)\nu_{Ij}\left(-5-10\nu_{Ij}^{\,n_{Ij}}+3\nu_{Ij}^{\,1+n_{Ij}}\right) \\ +3\left(-1-\nu_{Ij}-2\nu_{Ij}^{\,2}+4\nu_{Ij}^{\,1+n_{Ij}}-\nu_{Ij}^{\,2+n_{Ij}}+\nu_{Ij}^{\,3+n_{Ij}}\right) \end{pmatrix}$$

$$k_{j4} = C_j \begin{pmatrix} n_{Iy}^{\,2}\left(-1+\nu_{Ij}\right)^2\left(-4+\nu_{Ij}^{\,1+n_{Ij}}\right) \\ -n_{Ij}\left(-1+\nu_{Ij}\right)\left(-8+20\nu_{Ij}+5\nu_{Ij}^{\,1+n_{Ij}}+\nu_{Ij}^{\,2+n_{Ij}}\right) \\ +6\left(-1+2\nu_{Ij}-4\nu_{Ij}^{\,2}+\nu_{Ij}^{\,1+n_{Ij}}+\nu_{Ij}^{\,2+n_{Ij}}+\nu_{Ij}^{\,3+n_{Ij}}\right) \end{pmatrix}$$

$$k_{j5} = C_j \begin{pmatrix} 2n_{Ij}^{\,2}\left(-1+\nu_{Ij}\right)^2\left(-1+\nu_{Ij}^{\,1+n_{Ij}}\right) \\ +n_{Ij}\left(-1+\nu_{Ij}\right)\left(1-10\nu_{Ij}-10\nu_{Ij}^{\,1+n_{Ij}}+\nu_{Ij}^{\,2+n_{Ij}}\right) \\ +3\left(-1-\nu_{Ij}-4\nu_{Ij}^{\,2}+4\nu_{Ij}^{\,1+n_{Ij}}+\nu_{Ij}^{\,2+n_{Ij}}+\nu_{Ij}^{\,3+n_{Ij}}\right) \end{pmatrix}$$

$$k_{j6} = C_j \begin{pmatrix} n_{Ij}^{\,2}\left(-1+\nu_{Ij}\right)^2\left(-1+4\nu_{Ij}^{\,1+n_{Ij}}\right) \\ +n_{Ij}\left(-1+\nu_{Ij}\right)\left(-1-5\nu_{Ij}-20\nu_{Ij}^{\,1+n_{Ij}}+8\nu_{Ij}^{\,2+n_{Ij}}\right) \\ +6\left(-1-\nu_{Ij}-\nu_{Ij}^{\,2}+4\nu_{Ij}^{\,1+n_{Ij}}-2\nu_{Ij}^{\,2+n_{Ij}}+\nu_{Ij}^{\,3+n_{Ij}}\right) \end{pmatrix}$$

where $C_j = I_{jL}/\left[(1+n_{Ij})(2+n_{Ij})(3+n_{Ij})(-1+\nu_{Ij})^3\right]$; ν_{Ij} is the tapering ratio$\left(=\sqrt[n_{Ij}]{I_{jR}/I_{jL}}\right)$, and the subscript j defines the moments of inertia (I_y and I_z) and the warping constant (I_w).

8. Acknowledgments

The first author would like to acknowledge the financial support from the Competitive Research Projects, Postgraduate, Research, and Cultural Affairs Sector, Mansoura University, Egypt.

References

[1] G. Piana, E. Lofrano, A. Carpinteri, and G. Ruta, "Effect of local stiffeners and warping constraints on the buckling of symmetric open thin-walled beams with high warping stiffness," *Meccanica,* vol. 56, no. 8, pp. 2083-2102, 2021/08/01 2021.

[2] T. D. Dang, R. K. Kapania, and M. J. Patil, "Analytical Modeling of Cracked Thin-Walled Beams Under Torsion," *AIAA Journal,* vol. 48, no. 3, pp. 664-675, 2010/03/01 2010.

[3] W. Gao, A. H. A. Abdelrahman, S. W. Liu, and R. D. Ziemian, "Second-order dynamic time-history analysis of beam-columns with nonsymmetrical thin-walled steel sections," *Thin-Walled Structures,* vol. 160, p. 107367, 2021/03/01/ 2021.

[4] L. Chen, A. H. A. Abdelrahman, S. W. Liu, D. Ziemian Ronald, and S. L. Chan, "Gaussian Beam–Column Element Formulation for Large-Deflection Analysis of Steel Members with Open Sections Subjected to Torsion," *Journal of Structural Engineering,* vol. 147, no. 12, p. 04021206, 2021/12/01 2021.

[5] N. S. Trahair, "Lateral buckling of tapered members," *Engineering Structures,* vol. 151, pp. 518-526, 2017/11/15/ 2017.

[6] N. S. Trahair, "Trends in the code design of with initial lateral displacement," *Adv. Steel Construct.,* vol. 14, no. 1, p. 20, 2017.

[7] M. Kucukler and L. Gardner, "Design of laterally restrained web-tapered steel structures through a stiffness reduction method," *Journal of Constructional Steel Research,* vol. 141, pp. 63-76, 2018.

[8] M. Kucukler and L. Gardner, "Design of web-tapered steel beams against lateral-torsional buckling through a stiffness reduction method,"

Engineering Structures, vol. 190, pp. 246-261, 2019/07/01/ 2019.

[9] N. S. Trahair, "Inelastic lateral buckling of continuous steel beams," *Engineering Structures,* vol. 190, pp. 238-245, 2019/07/01/ 2019.

[10] R. Bai, S. W. Liu, and S. L. Chan, "Modal and Elastic Time-History Analysis of Frames with Tapered Sections by Non-Prismatic Elements," *International Journal of Structural Stability and Dynamics,* vol. 18, no. 09, 2018.

[11] R. Bai, S. W. Liu, Y. P. Liu, and S. L. Chan, "Direct analysis of tapered-I-section columns by one-element-per-member models with the appropriate geometric-imperfections," *Engineering Structures,* vol. 183, pp. 907-921, 2019.

[12] S. N. Chockalingam, V. Pandurangan, and M. Nithyadharan, "Timoshenko beam formulation for in-plane behaviour of tapered monosymmetric I-beams: Analytical solution and exact stiffness matrix," *Thin-Walled Structures,* vol. 162, p. 107604, 2021/05/01/ 2021.

[13] A. H. A. Abdelrahman, L. Chen, S. W. Liu, and R. D. Ziemian, "Timoshenko line-element for stability analysis of tapered I-section steel members considering warping effects," *Thin-Walled Structures,* vol. 175, p. 109198, 2022/06/01/ 2022.

[14] S. W. Liu, R. Bai, and S. L. Chan, "Second-order analysis of non-prismatic steel members by tapered beam–column elements," *Structures,* vol. 6, pp. 108-118, 2016.

[15] R. Bai, S. W. Liu, and S. L. Chan, "Finite-element implementation for nonlinear static and dynamic frame analysis of tapered members," *Engineering Structures,* vol. 172, pp. 358-381, 2018.

[16] W. L. Gao, A. H. A. Abdelrahman, S. W. Liu, and R. D. Ziemian, "Second-order dynamic time-history analysis of beam-columns with nonsymmetrical thin-walled steel sections," *Thin-Walled Structures,* vol. 160, p. 107367, 2021/03/01/ 2021.

[17] A. H. A. Abdelrahman, S. W. Liu, Y. P. Liu, and S. L. Chan, "Simulation of Thin-Walled Members with Arbitrary-Shaped Cross-Sections for Static and Dynamic Analyses," *International Journal of Structural Stability and Dynamics,* vol. 20, no. 12, 2020.

[18] S. W. Liu, W. L. Gao, and R. D. Ziemian, "Improved line-element formulations for the stability analysis of arbitrarily-shaped open-section beam-columns," *Thin-Walled Structures,* vol. 144, p. 106290, 2019.

[19] S. W. Liu, R. D. Ziemian, L. Chen, and S. L. Chan, "Bifurcation and large-deflection analyses of thin-walled beam-columns with non-symmetric open-sections," *Thin-Walled Structures,* vol. 132, pp. 287-301, 2018.

[20] A. H. A. Abdelrahman, S. Lotfy, and S. W. Liu, "Generalized Line-element Formulations for Geometrically Nonlinear Analysis of Nonsymmetric Tapered Steel Members with Warping and Wagner Effects," *Engineering Structures (Under review),* 2022.

[21] W. McGuire, R. Gallagher, and R. D. Ziemian, *Matrix Structural Analysis, John Wiley and Sons*. 2000.

[22] R. Ziemian, W. McGuire, and S. W. Liu, "MASTAN2 v5," ed, 2019.

[23] W. B. Yuan, B. Kim, and C. Chen, "Lateral–torsional buckling of steel web tapered tee-section cantilevers," *Journal of Constructional Steel Research,* vol. 87, pp. 31-37, 2013/08/01/ 2013.